Scientia Iranica B (2015) 22(3), 835–843

Sharif University of Technology
Scientia Iranica
Transactions B: Mechanical Engineering
www.scientiairanica.com

Numerical analysis of thermally developing turbulent flow in partially filled porous pipes

A. Nouri-Borujerdi* and **M.H. Seyyed-Hashemi**

School of Mechanical Engineering, Sharif University of Technology, Tehran, Iran.

Received 6 April 2014; received in revised form 24 July 2014; accepted 28 September 2014

KEYWORDS
Partially filled porous pipe flow;
Darcy-Brinkman-Forchheimer model;
Turbulent flow;
Numerical method with a single-domain approach.

Abstract. This work numerically simulates thermally developing turbulent flow in a partially filled porous pipe. The pipe is made up of a clear fluid region and a centering fluid-saturated porous medium region. The pipe is subjected to a constant wall temperature. Darcy-Brinkman-Forchheimer model is used to model the momentum equations in the porous medium. The effects of porous thickness and Darcy number on the pressure drop and heat transfer rate are investigated in the range of $0.2 \leq \delta/R < 1$ and $10^{-6} < \mathrm{Da} < 10^{-4}$ with the $k - \varepsilon$ turbulent model. It is found that when the thickness of the porous medium increases, the local Nusselt number along the pipe approaches a constant value corresponding to its fully developed conditions in a short thermal entrance length. In addition, when the Darcy number decreases, the fluid velocity inside the porous medium decreases, while the velocity outside the porous region increases at the expense of a reasonable pressure drop, which depends on the permeability of the porous matrix.

1. Introduction

The employment of different types of porous media in forced convection heat transfer has been extensively studied due to the wide range of potential engineering applications, such as heat pipe, electronic cooling, cross flow filtration, solid matrix heat exchangers and enhanced recovery of petroleum reservoirs. The numerical simulations of turbulent flow within the porous region can use either a microscopic or macroscopic model. The microscopic model provides more detailed insight into the flow structure, but only with simple geometry of porous media [1]. The macroscopic turbulent model describes the characteristics of fluid flow within a porous medium by volume-averaged variables. In addition, some required terms for fluid-particle interactions are incorporated in the momentum equations and turbulent models. The characteristics associated with the macroscopic modeling of turbulent flow through a partially filled porous pipe are not fully understood primarily due to lack of proper mathematical treatments of different regions and secondly due to the unspecified their interface boundary conditions [2].

Some papers have developed relations for turbulent flow inside porous media. Marcos and de Lemos [3] presented two different methodologies for developing turbulence models for flow in a porous medium. The first one starts with the macroscopic equations using the Forchheimer-extended Darcy model. The second method makes use of the Reynolds-averaged equations. These two methodologies lead to distinct set of equations for the $k - \varepsilon$ model. Antohe and Lage [4] presented a two-equation turbulence model for incompressible flow within a fluid saturated and rigid porous medium. The derivation consists of time-averaging the general (macroscopic) transport equations and closing the model with the classical eddy diffusivity concept and the Kolmogorov-Prandtl relation. The transport equations for the turbulence kinetic energy (k) and

*. *Corresponding author.*
E-mail address: anouri@sharif.ir (A. Nouri-Borujerdi)

its dissipation rate (ε) are attained from the general momentum equations. Macedo et al. [5] studied the influence of turbulence effects on a fluid flow through a (pseudo) porous media by numerically solving the set of Reynolds-averaged Navier-Stokes equations with the $k-\varepsilon$ turbulent model. The objective of this work was to access the behavior of the generalized friction factor with varying Reynolds number. Nakayama and Kuwahara [6] investigated the complete set of macroscopic two-equation turbulence model equations established for analyzing turbulent flow and heat transfer within porous media.

There are very few works that solve the turbulent flow in the partially filled porous pipes. Yang and Hwang [7] solved numerically turbulent flow in a partial porous pipe. The porous medium inserted at the middle of the pipe center. The numerical results show that the flow field can be adjusted and the thickness of boundary layer can be decreased by the inserted porous medium, so that the heat transfer can be enhanced in the pipe. The selection of the boundary conditions used at the interface between porous and clear fluid regions is very important in pipe flows [8-10]. Silva and de Lemos [11] solved turbulent flow in partially filled porous channels. They considered a jump condition in which shear stresses on both sides of the interface are not with the same value. They also investigated the effects of Reynolds number, porosity, permeability and jump coefficient on mean and turbulence fields. Cebeci [12] extended Van Driest's theory which provides continuous velocity and shear distributions in turbulent flow near a porous wall with pressure gradient.

Yang and Hwang [13] considered the numerical predictions on the turbulent flow and heat transfer characteristics for a rectangular channel with porous baffles which are arranged on the bottom and top of the channel walls in a periodically staggered way. They found that relative to the solid-type baffle channel, the porous-type baffle channel has a lower friction factor due to less channel blockage. Kumar et al. [14] analyzed the fully developed combined free and forced convective flow in a fluid saturated porous medium channel bounded by two vertical parallel plates, where the fluid flow was modeled using Brinkman equation model. By perturbation series method, they found that the presence of porous matrix reduces the velocity and temperature.

The objective of this study is to investigate the effect of a porous medium on the pressure drop and heat transfer rate of turbulent flow in a pipe with fully or partially filled porous medium under constant wall temperature. The $k-\varepsilon$ turbulent model is employed in an attempt to predict the turbulent shear stresses. The finite difference method based on the control volume approach is used for discretizing the governing equations with a single-domain technique. The set of algebraic discretized coupled equations are solved using SIMPLE algorithm. The effects of the porous thickness and Darcy number on the rate of heat transfer and pressure drop have been discussed.

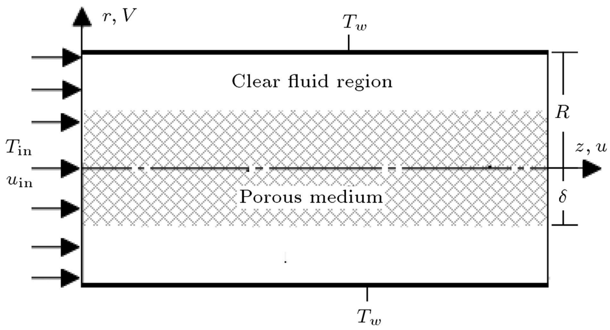

Figure 1. Schematic diagram of turbulent flow with a porous medium at the center of the pipe.

2. Problem statement and governing equations

This work considers a turbulent forced convective heat transfer in a partially filled porous pipe in which the porous medium is inserted at the core of the pipe, (Figure 1). A generalized equation known as the Brinkman-Forchheimer extended Darcy equation inside the porous medium region is solved numerically with one-domain approach along with the Navier-Stokes equations in the clear fluid region. In this approach, a single set of transport equations can be written for the entire domain comprising the homogeneous porous material and clear fluid regions with the interface between them as follows:

Mass equation:

$$\frac{\partial u}{\partial z}+\frac{1}{r}\frac{\partial (rv)}{\partial r}=0 \tag{1}$$

r-momentum equation:

$$\frac{\partial \rho uv}{\partial z}+\frac{1}{r}\frac{\partial r\rho v^2}{\partial r}=-\frac{dp}{dr}+\frac{\partial}{\partial r}\left[(\mu+f\mu_t)\frac{1}{r}\frac{\partial rv}{\partial r}\right]+\frac{\partial}{\partial z}\left[(\mu+f\mu_t)\frac{\partial v}{\partial z}\right]-\phi\frac{\mu v}{K}+\phi^2\frac{C_F\rho|v|v}{\sqrt{K}}. \tag{2}$$

z-momentum equation:

$$\frac{\partial \rho u^2}{\partial z}+\frac{1}{r}\frac{\partial r\rho uv}{\partial r}=-\frac{dp}{dz}+\frac{1}{r}\frac{\partial}{\partial r}\left[(\mu+f\mu_t)r\frac{\partial u}{\partial r}\right]+\frac{\partial}{\partial z}\left[(\mu+f\mu_t)\frac{\partial u}{\partial z}\right]-\phi\frac{\mu u}{K}+\phi^2\frac{C_F\rho|u|u}{\sqrt{K}}. \tag{3}$$

u and v are the average velocity components of the fluid over a volume element of fluid in r- and z-direction, respectively. ϕ is the porosity of the porous material defined as ratio of the void to the total volume. K is an empirical constant, called permeability of the medium (in general, a second order tensor), and is usually taken to be constant. The coefficient μ is the effective viscosity of the porous medium and is not, in general, the fluid viscosity. However, many authors, including Brinkman himself, Antohe and Lage [4] used the same fluid viscosity for μ, although Givler and Altobelli [15] suggested the effective viscosity can deviate substantially from the fluid viscosity. μ_t denotes turbulent viscosity and f is defined as a binary constant. If $f = 1$ and $K \to \infty$, Eqs. (2) and (3) changes to the Navier-Stokes equations and are applicable for the clear fluid region. If $f = 0$, K = finite and $0 < \phi < 1$, in this case, Eqs. (2) and (3) reduces to the Brinkman-Forchheimer extended Darcy equations and are suitable for the porous region.

Turbulent flow in a porous medium is a controversial issue. With very small permeability and fluid velocity, the flow is often dominated by the laminar flow regime. But, with high-speed flow through a highly permeable medium, the flow can lead to a turbulent flow therein. In modeling of energy equation, it is assumed that the local thermal equilibrium exists between solid and fluid phase in the porous region as Kaviany [16] adopted. The work of Mohamad and Karim [17] reveals that the thermal equilibrium assumption is valid as far as there is no heat released in the porous region. Moreover, a few tests with two energy equations by Mohamad [18] indicate that the results are not sensitive to the non-equilibrium conditions for $\mathrm{Nu}(= h_v D^2/k)$ of 100. For $\mathrm{Nu} = 10$ the difference is less than 1%.

Therefore, the energy equation of the partially filled porous pipe including the clear fluid region as well as the porous region will be given as:

$$\frac{\partial uT}{\partial z} + \frac{1}{r}\frac{\partial rvT}{\partial r} = \frac{1}{r}\frac{\partial}{\partial r}\left[(\alpha + f\alpha_t) r \frac{\partial T}{\partial r}\right] + \frac{\partial}{\partial z}\left[(\alpha + f\alpha_t)\frac{\partial T}{\partial z}\right]. \tag{4}$$

If $f = 1$, the energy equation is applicable for the clear fluid region and its turbulent thermal diffusivity is defined as $\alpha_t = \nu_t / \mathrm{Pr}_t$ in which Pr_t is the turbulent Prandtl number. As $f = 0$, the energy equation is used for the porous region with $\alpha = [\phi k_f + (1-\phi)k_s]/\rho_f c_f$. k is thermal conductivity and subscripts f and s refer to the fluid and solid phases, respectively.

3. Tubulence modeling

For turbulence modeling, the $k-\varepsilon$ model is adopted as follows:

$$\frac{\partial uK}{\partial z} + \frac{1}{r}\frac{\partial rvK}{\partial r} = \frac{\partial}{\partial z}\left[\frac{\nu_t}{\sigma_k}\frac{\partial K}{\partial z}\right] + \frac{1}{r}\frac{\partial}{\partial r}\left[r\frac{\nu_t}{\sigma_k}\frac{\partial K}{\partial r}\right] + G - \varepsilon, \tag{5}$$

$$\frac{\partial u\varepsilon}{\partial z} + \frac{1}{r}\frac{\partial rv\varepsilon}{\partial r} = \frac{\partial}{\partial z}\left[\frac{\nu_t}{\sigma_\varepsilon}\frac{\partial \varepsilon}{\partial z}\right] + \frac{1}{r}\frac{\partial}{\partial r}\left[r\frac{\nu_t}{\sigma_\varepsilon}\frac{\partial \varepsilon}{\partial r}\right] + C_{1\varepsilon}\frac{\varepsilon}{k}G - C_{2\varepsilon}\frac{\varepsilon^2}{K}, \tag{6}$$

and the turbulent eddy viscosity can be determined by:

$$\nu_t = C_\mu \frac{K^2}{\varepsilon}. \tag{7}$$

where G is called the production term and is derived from:

$$G = -\rho\overline{u_i' u_j'}.E_{ij} = \frac{\mu_t}{2}\left[\frac{\partial u_i}{\partial x_j} + \frac{\partial u_j}{\partial x_i}\right]\frac{\partial u_j}{\partial x_i} = \mu_t\left\{\left[\frac{\partial u}{\partial z}\right]^2 + \left[\frac{\partial v}{\partial r}\right]^2 + \left[\frac{v}{r}\right]^2 + \frac{1}{2}\left[\frac{\partial u}{\partial r} + \frac{\partial v}{\partial z}\right]^2\right\}. \tag{8}$$

Eqs. (5), (6) and (7) contain five adjustable constant σ_k, σ_ε, $C_{1\varepsilon}$, $C_{2\varepsilon}$ and C_μ.

4. Boundary conditions

The required boundary conditions for the above governing equations, i.e. in the clear fluid region as well as in the porous region are specified as follows:

$$u(0;r) = u_{\mathrm{in}}, \qquad v(0;r) = 0, \qquad T(0;r) = T_{\mathrm{in}}, \tag{9a}$$

$$K(0,r) = \frac{3}{2}(0.05u_{\mathrm{ref}})^2, \qquad \varepsilon(0,r) = \frac{C_\mu^{\frac{3}{4}} K^{\frac{3}{2}}}{0.035D}, \tag{9b}$$

$$\frac{\partial \psi(L,r)}{\partial z} = 0, \qquad \text{where} \quad \psi = [u, v, T, K, \varepsilon]^T, \tag{9c}$$

$$\frac{\partial \psi(z,0)}{\partial r} = 0, \qquad \text{where} \quad \psi = [u, T, K, \varepsilon]^T,$$

$$v(z,0) = 0, \tag{9d}$$

$$u(z,R) = 0, \qquad v(z,R) = 0, \qquad T(z,R) = T_w. \tag{9e}$$

4.1. Near-wall boundary condition

To obtain an accurate solution for the turbulent flow, many grid points are required to be taken inside the linear sub-layer, so that the grid spacing being so fine as to be uneconomical. Thereby, the near-wall region may be sub-divided into three different areas, viscous sub-layer, buffer layer and inertial sub-layer [19]. In the buffer layer, however, both turbulent and viscous effects are of importance [20]. Instead of trying to model the behavior in the buffer layer, the common practice is to place the first near-wall node in either the viscous sub-layer for low Reynolds number, or in the inertial sub-layer for high Reynolds number. The functions that bridge the near-wall region between the wall and the first near-wall node is linear function in the viscous sub-layer or wall function in the inertial sub-layer region. In the present work, we assume the air flow in the porous region is laminar and in the clear fluid region is turbulent flow with high Reynolds number. The nearest grid point from the wall is assumed to be in the range of $30 < yu_\tau/\nu < 200$. The corresponding wall function is given as follows [21]:

$$u = \frac{u_\tau}{\kappa}\ln(9.8yu_\tau/\nu),$$

$$\frac{(T_w - T)\rho c_p u_\tau}{q_w} = 2.187\ln(yu_\tau/\nu) + 3.8, \tag{10a}$$

$$K_{\text{source}} = \frac{\tau_w u - \rho C_\mu^{\frac{3}{4}} K^{\frac{3}{2}} u^+}{y}, \qquad K = \frac{u_\tau^2}{\sqrt{C_\mu}},$$

$$\varepsilon = \frac{u_\tau^3}{\kappa y^+}, \tag{10b}$$

$$\tau_w = \frac{\rho C_\mu^{\frac{1}{4}} K^{\frac{1}{2}} u}{u^+}, \qquad u_\tau = \sqrt{\frac{\tau_w}{\rho}}, \tag{10c}$$

where, $\kappa = 0.41$.

The Nusselt number between the air flow and the pipe surface under wall constant temperature will be obtained from

$$\mathrm{Nu} = \frac{q_w D}{k_f(T_w - T_m)} = \frac{\mathrm{Pe}}{T_m^+ u_m^+}. \tag{11}$$

T_m is the fluid average temperature, and $\mathrm{Pe} = u_m D/\alpha$ is the Peclet number.

5. Numerical procedure

The numerical solution of the governing equations may be accomplished by employing either of one- or two-domain approach [22,23]. One of the major difficulties of numerical solution at the interface between the clear flow and the porous medium in the one-domain approach is large changes of porous parameters, such as porosity and permeability. Consequently, the model equations require special treatment at the interface region. Although, the experimental results of Basu and Khalili [24] show that a one-domain approach can provide good predictions of interfacial flow. The interface can be either a continuous transition zone across which the physical variables encounter possibly strong but nevertheless continuous variations [25] or a discontinuous interface where the physical variables are possibly discontinuous [26-28]. Arquiset et al. [29] used a harmonic mean formulation of the permeability, and Poulikakos [30] used a hyperbolic tangent function to handle the abrupt change in governing parameters.

In this study, to obtain the flow parameters in the clear flow and the fluid-saturated porous regions, the governing equations (Eqs. (1)-(7)) along with boundary conditions (Eqs. (9a)-(9e)) have been solved numerically in one-domain approach by finite difference technique and SIMPLE algorithm. Discretization of the governing equations was accomplished on the staggered grid arrangement with uniform grid spacing in r- and z-directions. The second order upwind differencing scheme was used for convection terms and the central differencing scheme for diffusion terms. Subsequently, the discretized linear algebraic equations for u, v and p were solved using successive line-by-line relaxation by tri-diagonal matrix algorithm. Either of the algebraic equations included only three non-zero coefficients. We also used a hyperbolic tangent function to handle the abrupt change in governing parameters including porosity and permeability. The convergence criterion for solution of equations was established by locally and globally mass and energy conservations in which their corresponding residuals were set equal to 10^{-6}.

6. Result and discussion

A uniform air flow enters a pipe at velocity of 3.905 m/s and at temperature of 25°C (Figure 1). The pipe is with diameter of 4 cm and length of 50 cm under constant surface temperature of 35°C. The porous material is assumed to be made of aluminum with physical properties of $\rho = 2770$ kg/m^3, $k = 177$ w/m.k, and porosity, $\phi = 0.7$. In the single domain approach, the generalized equations (Eqs. (1)-(4)) can be used for the porous region if $f = 0$, $\phi < 1$ and $K =$ finite, and they are reduced to the clear flow conditions if the porous matrix disappears, that is $f = 1$ and $K \to \infty$. The single domain approach proposed by Choi and Waller [31] and employed by Chan et al. [2] can be used to solve the fluid/porous interface problems by appropriately changing the properties of the porous medium in the computational domain. We used here a hyperbolic tangent function to handle the properties changes at the interface.

6.1. Model tests

To validate the numerical results and mesh size independency, some mesh refinement is tested. To compare the present results with the previous works published in open literature, some validations are accomplished. In this regard, Figure 2 shows the fully developed pressure gradient for four different mesh sizes of 6×11, 11×21,

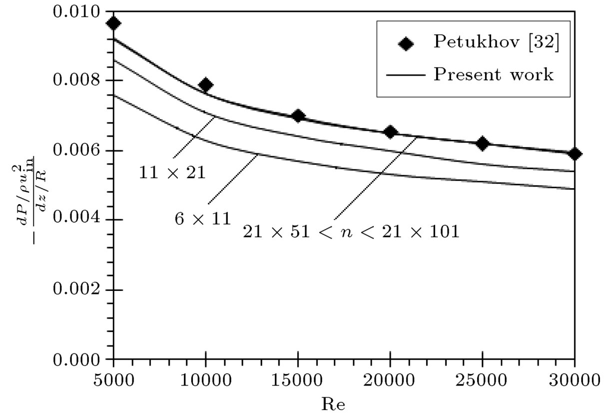

Figure 2. Effect of mesh refinement on fully developed pressure gradient and data of Petukhov [32].

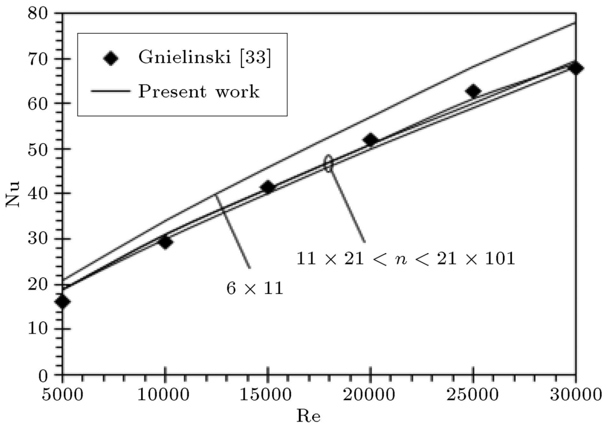

Figure 3. Effect of mesh refinement on fully developed Nusselt number and data of Gnielinski [33].

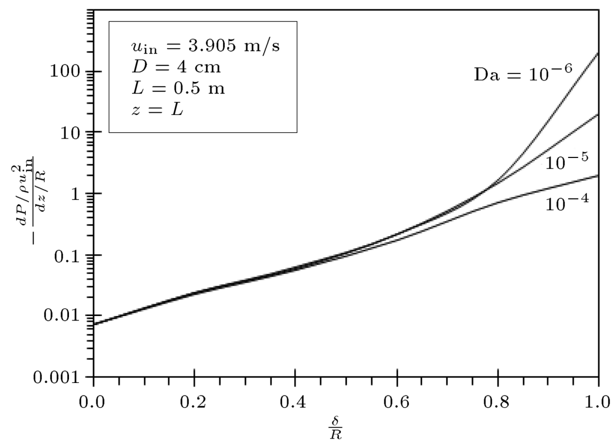

Figure 4. Effect of Darcy number on fully developed pressure gradient vs. the porous radius.

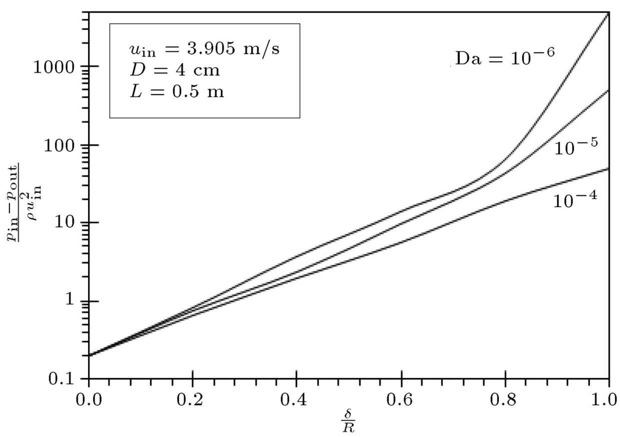

Figure 5. Effect of Darcy number on total pressure drop vs. the porous radius.

21×51 and 21×101 as well as the data of Petukhov [32]. These results refer only to the fully developed turbulent air flow in a clear pipe, without porous medium because there was not any available data in open literature for comparison with turbulent flow in the clear flow or laminar flow in the porous region. Figure 3 depicts the fully developed Nusselt number against Reynolds number for different mesh sizes of 6×11 and $11\times21 < n < 21\times101$ as well as the data of Gnielinski [33]. Comparison between the present results and the data of Petukhov and Gnielinski gives a satisfactory agreement among them. Thereby, 21×101 computational nodes were selected in r- and z-directions respectively for the next numerical calculations.

Figures 4 and 5 show the effect of Darcy number, $\mathrm{Da} = K/D^2$, on the fully developed pressure gradient at the outlet cross section of the pipe versus the porous thickness. The pressure gradient on the ordinate axis has been dimensionless by the inlet fluid velocity. By decreasing the Darcy number, the pressure drop increases, because the porous medium with low permeability resists against the fluid flow. Moreover, the effect of Darcy number on the pressure drop is more prominent when the porous thickness is increasing, in particular when $\delta/R > 0.8$. The reason is that the fluid is pushed towards the pipe wall and causes an increase in the speed of the fluid.

Figure 6 illustrates the effect of porous thickness on the fully developed axial velocity profile in the pipe at the outlet cross section for $\mathrm{Da} = 10^{-4}$. The figure indicates the velocity for five different porous thicknesses (radius), $\delta/R = 0$, 0.2, 0.4, 0.6 and 0.8. The velocity profile in the clear flow region is a turbulent flow and in the porous region is a Darcy flow with a uniform distribution. As the thickness of the porous medium is increasing, more fluid flows between the porous region and the pipe wall with a maximum velocity of the fluid shifts toward the surface of wall. When δ/R approaches zero, the porous matrix disappears in the pipe and the entire region is occupied by the clear flow with a turbulent flow regime.

Figure 6 has been reproduced in Figure 7 for $\mathrm{Da} = 10^{-6}$. It is observed that the shape of the velocity profiles is the same as the velocity profiles in Figure 6. As the Darcy number decreases, the fluid

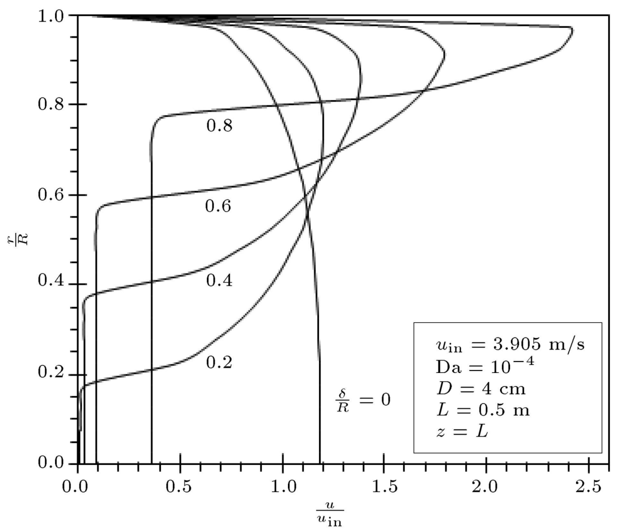

Figure 6. Effect of porous radius on fully developed axial velocity of the pipe for Da $= 10^{-4}$.

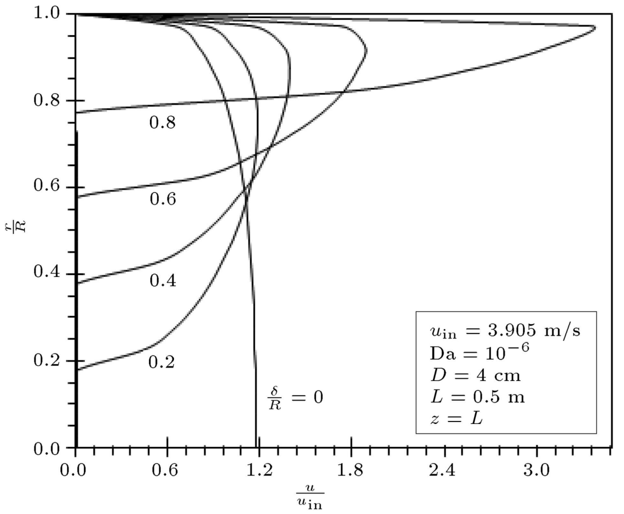

Figure 7. Effect of porous radius on fully developed axial velocity of the pipe for Da $= 10^{-6}$.

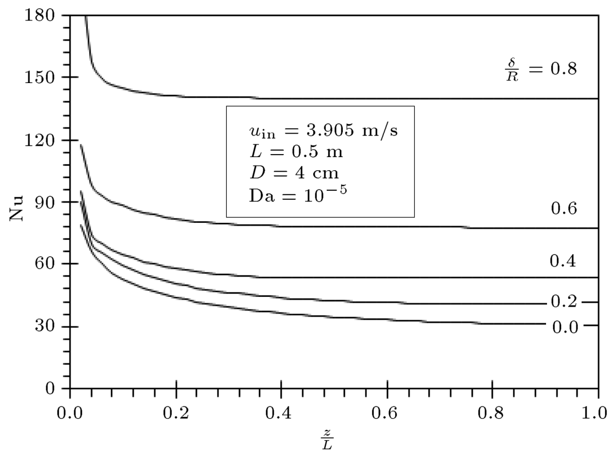

Figure 8. Effect of porous radius on developing Nusselt number along the pipe for Da $= 10^{-5}$.

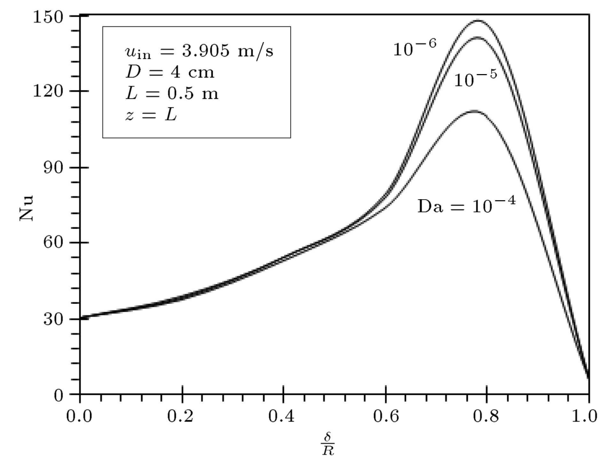

Figure 9. Effect of Darcy number on fully developed Nusselt number vs. the porous radius.

velocity inside the porous medium decreases, while the velocity outside the porous region increases. For example, when the porous thickness is $\delta/R = 0.8$, the value of the fluid velocity drops from 0.36 in Figure 6 to zero in Figure 7. The decrease in the Darcy number forces the porous medium to resists against the fluid flow. The trend of the velocity profiles in Figures 6 and 7 of the present work are exactly the same as the velocity profiles in Figure 8(a) and (b) of Pavel [34] for Re = 100, Da $= 10^{-3}$ and Da $= 10^{-6}$, respectively.

Figure 8 depicts the effect of porous thickness on the developing Nusselt number along the pipe for Da $= 10^{-5}$. Either curve approaches a constant value corresponding to their fully developed conditions in a short thermal entrance length. In other words, the thermal entrance length decreases when the porous thickness increases. For instance, the thermal entrance length decreases from about $Z/L = 0.5$ to 0.2 when the porous thickness increases from $\delta/R = 0.0$ to 0.8. The enhancement of the Nusselt number can be explained by the fact that as more fluid is pushed towards the pipe wall by the porous medium, the hydrodynamic boundary layer thickness becomes thinner next to the wall, and more momentum and energy fluxes can exchange therein due to the speed of the fluid. This result can be observed by the experimental data of Pavel [35].

Figure 9 presents the effect of Darcy number on the fully developed Nusselt number at the outlet cross section of the pipe. The porous thickness can increase the Nusselt number progressively up to $\delta/R = 0.8$, then it drops sharply. The reason is that the effect of Darcy number is more significant when the porous material is thickening and more fluid is passing over the surface wall. The figure also shows that when $\delta/R > 0.8$, a large part of the pipe, being blocked by the porous material, results in lower flow rate and then the Nusselt number decreases regardless of the value of Darcy number.

7. Conclusions

Forced convection turbulent flow and heat transfer has been numerically investigated in a partially filled porous pipe in a single-domain approach. The effects of porous thickness and Darcy number are investigated with $k-\varepsilon$ turbulent model. As the thickness of the porous medium increases, the local Nusselt number along the pipe approaches a constant value corresponding to its fully developed conditions in a short thermal entrance length. In other words, the thermal entrance length decreases when the porous thickness increases. For instance, the thermal entrance length decreases from about $Z/L = 0.5$ to 0.2 when the porous thickness increases from $\delta/R = 0.0$ to 0.8. In addition, when the Darcy number decreases, the fluid velocity inside the porous medium decreases, while the velocity outside the porous region increases at the expense of a reasonable pressure drop, which depends on the permeability of the porous matrix.

Nomenclature

C_p	Specific heat
C_F	Forchheimer coefficient
D	Pipe diameter
Da	Darcy number, K/D^2
G	Generation
f	Binary constant
h	Heat transfer coefficient
k	Thermal conductivity, permeability
K	Turbulent kinetic energy
L	Pipe length
Nu	Nusselt number, hd/k
p	Pressure
Pe	Peclet number, $u_m D/\alpha$
$\dot{q}$	Heat flux
r	Radial coordinate
R	Inside pipe radius
Re	Reynolds number, $u_m D/\nu$
T	Temperature
u	Axial velocity
v	Radial velocity
y	Measured from the wall
z	Axial coordinate
y^+	$y\sqrt{\tau_w/\rho}/\nu$
T^+	$(T_w - T)C_p\rho u_\tau/\dot{q}_w$

Greek letters

α	Thermal diffusivity
δ	Thickness of porous media
ε	Turbulence dissipation rate
ϕ	Porosity
μ	Dynamic viscosity
ν	Kinematic viscosity
ρ	Density
τ	Shear stress

Subscripts

f	Fluid
in	Inlet
m	Average
p	Particle
t	Turbulent
w	Wall

References

1. Prinos, P., Sofialidis, D. and Keramaris, E. "Turbulent flow over and within a porous bed", *Journal of Hydraulic Engineering*, **129**(9), pp. 720-733 (2003).
2. Chan, H.C., Huang, W.C., Leu, J.M. and Lai, C.J. "Macroscopic modeling of turbulent flow over a porous medium", *Int. J. of Heat and Fluid Flow*, **28**, pp. 1157-1166 (2007).
3. Marcos, Pedras H.J. and de Lemos, M.J.S. "Macroscopic turbulence modeling for incompressible flow through undeformable porous media", *Int. J. of Heat and Mass Transfer*, **44**(8), pp. 1081-1093 (2001).
4. Antohe, B.V. and Lage, J.L. "A general two-equation macroscopic turbulence model for incompressible flow in porous media", *Int. J. Heat and Mass Transfer*, **40**(13), pp. 3013-3024 (1997).
5. Macedo, H.H., Costa, U.M.S. and Almeida, M.P. "Turbulent effects on fluid flow through disordered porous media", *Physica A-Statistical Mechanics and Applications-PHYSICA A*, **299**(3), pp. 371-377 (2001).
6. Nakayama, A. and Kuwahara, F. "A Macroscopic turbulence model for flow in a porous medium", *Journal of Fluids Engineering*, **121**(2), pp. 427-433 (June 1999).
7. Yang, Yue-Tzu and Hwang, Ming-Lu "Numerical simulation of turbulent fluid flow and heat transfer characteristics in heat exchangers fitted with porous media", *Int. J. of Heat and Mass Transfer*, **52**(1), pp. 2956-2965 (2009).
8. Alazmi, B. and Vafai, K. "Analysis of fluid flow and heat transfer interfacial conditions between a porous medium and a fluid layer", *Int. J. of Heat and Mass Transfer*, **44**(9), pp. 1735-1749 (2001).

9. Tan, H., Chen, X., Pillai, K.M. and Papathanasiou, T.D. "Evaluation of boundary conditions at the clear-fluid and porous-medium interface using the boundary element method", *Proceedings of the 9th Int. Conf. on Flow Processes in Composite Materials, (FPCM-9)*, Montréal (Québec), Canada (8-10 July 2008).

10. Tan, H. and Pillai, K.M. "Finite element implementation of stress-jump and stress-continuity conditions at porous-medium, clear-fluid interface", *Computers & Fluids*, **38**(6), pp. 1118-1131 (2009).

11. Silva, R.A. and de Lemos, M.J.S. "Turbulent flow in a channel occupied by a porous layer considering the stress jump at the interface", *Int. J. of Heat and Mass Transfer*, **46**(26), pp. 5113-5121 (2003b).

12. Cebeci, T. "Behavior of turbulent flow near a porous wall with pressure gradient", *AIAA Journal*, **8**(12), pp. 2152-2156 (1970).

13. Yang, Yue-Tzu and Hwang, Chih-Zong "Calculation of turbulent flow and heat transfer in a porous-baffled channel", *Int. J. of Heat and Mass Transfer*, **46**(5), pp. 771-780 (Feb. 2003).

14. Kumar, J.P., Umavathi, J.C., Pop, I. and Biradar, B.M. "Fully developed mixed convection flow in a vertical channel containing porous and fluid layer with isothermal or isoflux boundaries", *Transp. Porous Media*, **80**, pp. 117-135 (2009).

15. Givler, R.C. and Altobelli, S.A. "A determination of the effective viscosity for the Brinkman-Forchheimer flow model", *J. of Fluid Mechanics*, **28**, pp. 355-370 (1994).

16. Kaviany, M. "Laminar flow through a porous channel bounded by isothermal parallel plates", *Int. J. Heat Mass Trans.*, **28**, pp. 851-858 (1985).

17. Mohamad, A.A. and G.A, Karim "Flow and heat transfer within segregated beds of solid particles", *J. Porous Media*, **4**(3), pp. 215-224 (2001).

18. Mohamad, A.A. "Heat transfer enhancements in heat exchangers fitted with porous media, Part I: Constant wall temperature", *Int. J. of Thermal Science*, **42**, pp. 385-395 (2003).

19. Tennekes, H. and Lumley, J.L., *A First Course in Turbulence*, Massachusetts Institute of Technology, Cambridge (1972).

20. Sahay, A. and Sreenivasan, K.R. "The wall-normal position in pipe and channel flows at which viscous and turbulent shear stresses are equal", *Physics of Fluids*, **11**, pp. 3186-3188 (1993).

21. Wilcox, D.C. *Turbulence Modeling for CFD, DCW Industries*, Inc. La Canada, California (1994).

22. Jamet, D., Chandesris, M. and Goyeau, B. "On the equivalence of the discontinuous one- and two-domain approach for modeling of transport phenomena at a fluid/porous interface", *Transport in Porous Media*, **78**, pp. 403-418 (2009).

23. Beckermann, C. and Viskanta, R. "Double-diffusive convection during dendritic solidification of a binary mixture", *Physico Chem., Hydrodyn*, **10**, pp. 195-213 (1988).

24. Basu, A.J. and Khalili, A. "Computation of flow through a fluid-sediment interface in a benthic chamber", *Physics of Fluids*, **11**(6), pp. 1395-1405 (1999).

25. Valdes-Parada, F.J., Goyeau, B. and Ochoa-Tapia, J.A. "Diffusive mass transfer between a microporous medium and a homogeneous fluid: Jump boundary conditions", *Chem. Eng. Sci.*, **61**(5), pp. 1692-1704 (2006).

26. Silva, R.A. and de Lemos, M.J.S. "Numerical analysis of the stress jump interface conditions for laminar flow over a porous layer", *Numerical Heat Transfer, Part A*, **43**(6), pp. 603-617 (2003a).

27. Rashidi, S., Nouri-Borujerdi, A., Valipour, M.S., Ellahi, R. and Pop, I. "Stress jump and continuity conditions for a cylinder embedded in a porous medium", *Transport in Porous Media* (2014). DOI 10.1007/s11242-014-0431-3

28. Ehrhardt, M. "An introduction to fluid-porous interface coupling" (October 2010), http://www.math.uni-wuppertal.de.

29. Arquiset, E., Caltagirone, J.P. and Langlais, C. "Natural convection in cavities partially filled with permeable porous materials", *Proceedings of the 8th Int. Heat Transfer Conf.*, **2**, p. 2653 (1986).

30. Poulikakos, D. "Thermal instability in a horizontal fluid layer superposed on a heat generating porous bed", *Numerical Heat Transfer*, **12**, pp. 83-99 (1987).

31. Choi, C.Y. and Waller, P.M. "Momentum transport mechanism for water flow over porous media", *J. Environmental Engineering*, **123**(8), pp. 792-799 (1997).

32. Petukhov, B.S. "Heat transfer and friction in turbulent pipe flow with variable physical properties", *Advances in Heat Transfer*, **6**, Eds. T.F. Irvine and J.P. Hartnett, Academic Press, New York (1970).

33. Gnielinski, V. "New equations for heat and mass transfer in turbulent pipe and channel flow", *Int. Chemical Engineering*, **16**, pp. 359-368 (1976).

34. Pavel, B.I. and Mhamad, A.A. "An experimental and numerical study on heat transfer enhancement for gas heat exchangers fitted with porous media", *Int. J. of Heat and Mass Transfer*, **47**, pp. 4939-4952 (2004).

35. Pavel, B.I. and Mhamad, A.A. "experimental investigation of the potential of metallic porous inserts in enhancing forced convective heat transfer", *Trans. of the ASME, J. of Heat Transfer*, **126**, pp. 540-545 (Aug. 2004).

Biographies

Ali Nouri-Borujerdi is Professor of Mechanical Engineering at Sharif University of Technology, Tehran,

Iran, where he teaches undergraduate and graduate level courses in the Thermal/Fluids Sciences Group of the Mechanical Engineering Department. His teaching focuses on heat transfer, computational fluid dynamics and two-phase flows, including boiling and condensation. His current research programs include numerical simulation of two-phase flow, compressible turbulent flows and porous media. Professor Nouri has published more than 130 articles in international journals and conferences.

M.H. Seyyed-Hashemi received his BS in Mechanical Engineering from Iranian University of Sciences and Technology. His MS degree is in Thermal Fluid Sciences at the Department of Mechanical Engineering from Sharif University of Technology, Tehran, Iran.